Nanomed J. 12: 1-, 2025

RESEARCH PAPER

Influence of chitosan/gelatin/zinc oxide nanoparticles on mechanical and biological properties of three-dimensional scaffolds for tissue engineering

Parasto Hadaddi [1], ***Azadeh Asefnejad*** [1]*

[1]*Department of Biomedical Engineering, Science and Research Branch, Islamic Azad University, Tehran, Iran*

ABSTRACT

Objective(s): Herein, we investigated the effect of zinc oxide nanoparticles on the mechanical and biological properties of a three-dimensional (3D) scaffold.

Materials and Methods: The scaffolds were printed using chitosan and different ratios of gelatin and coated with sodium alginate and different ratios of nanoparticles. Morphology was examined using optical microscope and scanning electron microscope (SEM); and element specification was done using element identification analysis and element spotting (EDS and Map, repectively). The percentage of swelling and biodegradability was investigated by placing the samples in phosphate buffered salt solution. Fourier transform infrared spectroscopy (FTIR) was used to investigate functional groups. The mechanical properties of the scaffolds were determined using the tensile test and their biological properties were determined using the biocompatibility and percentage of cell viability.

Results: SEM images showed that the pores were filled during the printing proces due to the concentration and viscosity of the materials. Amide I, Amide III, and NH groups were detected by FTIR analysis. The highest swelling for 1Cs:3G and 1Cs:1G /0.5ZnO scaffolds was 392 and 154%, respectively. The highest degradability in 15 days was obtained for 1Cs:1G/0.5ZnO scaffold as 58%. The tensile strength and Young's modulus for 1Cs:1G/0.5Zn scaffold were 77.07 MPa and 61.2 MPa, respectively. prolonged drug release profiles with implants, scaffolds, and hydrogels.

Conclusion: The percentage of cell survival for 1Cs:1G/0.5ZnO scaffold was 98.44%. According to the studies, 1Cs:1G/0.5ZnO scaffold has good biological and mechanical properties, presenting it as a useful candidate for tissue engineering.

Keywords: *Biological properties, Mechanical properties, Three-dimensional scaffold, Tissue engineering, Zinc oxide nanoparticles*

How to cite this article

Hadaddi P, Asefnejad A. Influence of chitosan/gelatin/zinc oxide nanoparticles on mechanical and biological properties of three-dimensional scaffolds for tissue engineering. Nanomed J. 2025; 12(1): 1-. DOI: 10.22038/NMJ.2025.77558.1892

INTRODUCTION

Tissue engineering aims to regenerate and repair damaged tissues and organs by utilizing cells, biomaterials, and suitable biochemical and physical factors. Scaffolds play a crucial role in tissue engineering by providing a supportive structure for cell attachment, proliferation, and formation of new tissue [1-3]. The ideal scaffold should possess appropriate mechanical properties, biocompatibility, biodegradability, porosity, and surface chemistry to mimic the native extracellular matrix [4-5]. Gelatin and chitosan are naturally-derived polymers that have been widely used in biomedical fields due to their excellent biocompatibility and degradability. However, there is a need to improve their mechanical properties for tissue engineering scaffolds [4-6]. Zinc oxide nanoparticles are known for their antimicrobial properties and proven biosafety. Three-dimensional (3D) printing enables the fabrication of scaffolds with controlled architectures and intricate designs that are difficult to achieve using conventional techniques [7-9].

Polymers are large molecules composed of repeating structural units connected by covalent chemical bonds. Interest in using biological scaffolds for tissue engineering has increased in recent years. However, optimization is needed to ensure tissues

* *Corresponding author: Email: Asefnejad@srbiau.ac.ir*

Note. This manuscript was submitted on January 17, 2024; approved on May 8, 2024

effectively grow on the scaffold [10-13]. Chitosan is a natural polymer derived from chitin by partial deacetylation. It has unique bioactive properties like biocompatibility, biodegradability, wound healing, and so on, making it promising for tissue engineering. Chitosan is mainly extracted from exoskeletons of crustaceans like shrimp, crab, and insects through deacetylation using chemical or biological methods or a combination of them [14-19]. Degree of deacetylation, molecular weight, purity, and processing methods influence chitosan properties. Commonly used chitosans have 70-90% deacetylation. Chitosan shows antimicrobial activity against bacteria and fungi due to its polycationic structure [17-21]. Higher molecular weight and deacetylation degree enhance its antimicrobial activity. It acts as an antioxidant by scavenging free radicals via reactive groups. Higher molecular weight if chitosan exhibits better radical scavenging ability [20-25]. Other bioactivities include biocompatibility, non-toxicity, hemostatic, and wound healing promotion, making it promising for tissue engineering applications [26-28].

The aim of this study is to develop composite scaffolds made of gelatin, chitosan, and zinc oxide nanoparticles for bone tissue engineering using 3D printing [28-31]. We evaluate the physical, mechanical, and biological properties of the scaffolds. Our hypothesis is that adding zinc oxide nanoparticles will enhance the mechanical strength of the gelatin/chitosan scaffolds. Furthermore, 3D printing will enable us to create scaffolds with the necessary porosity and interconnected pores required for tissue regeneration. This research explores the potential of using a composite system consisting of natural polymers and nanoparticles along with 3D printing for applications in bone tissue engineering.

MATERIALS AND METHODS

For this study, biocompatible materials were obtained from specific suppliers. Chitosan and gelatin were sourced from Sigma-Aldrich and Merck, respectively. Acetic acid from Scharlau was used to prepare the chitosan bioink. DNA-biotech provided the phosphate buffer solution with a pH of 7.3 for swelling studies. Ethanol (C_{2H5OH}) was purchased from Scharlau. Distilled water from Zellal (Iran) was used for preparing the gelatin bioink and conducting swelling studies.

Scaffold Fabrication

Bioinks were prepared by dissolving 10% w/v chitosan in a 5% acetic acid solution and 12% w/v gelatin in distilled water. The scaffolds were designed using computer-aided design (CAD) software and fabricated using a 3D bioprinter (3DPL, N2) at room temperature. The printing process involved a print speed of 120 mm/sec, a pressure of 6 bar, and a print bed temperature of 10°C. The scaffolds were made with the different ratios of chitosan to gelatin, and they were then coated with a 1% sodium alginate solution. Zinc oxide nanoparticles were added at concentrations of 0.5%, 1.5%, and 3% to coat the scaffolds labeled as D, E, and F, respectively. Afterwards, the scaffolds were immersed in a 5% calcium chloride solution and air-dried for 24 hours at room temperature before being characterized.

Scaffold Characterization

The morphology of the fabricated scaffolds was initially observed using an optical microscope (MP-bell, Bell/Italy). The surface morphology and pore size were analyzed using a scanning electron microscope (SEM) (AIS2100, SERONTECHNOLOGIES), and the pore size was measured using ImageJ software. Fourier transform infrared (FTIR) spectroscopy (SRG 1100G) was used to identify the functional groups present in the scaffolds. The swelling behavior of the scaffolds was studied by immersing them in phosphate buffer solution (pH 7.3) for 30 hr and tracking the weight gain. Degradation studies were performed by incubating the scaffolds in phosphate buffer for 15 days and monitoring the weight loss. The mechanical properties, including tensile strength, modulus, and elongation at break, were evaluated using a universal testing machine (SMT-20) following ISO 6824 specifications.

The tensile test is a destructive testing method wherein a sample is subjected to uniaxial tension until it reaches its breaking point. Simultaneously, the elongation of the sample is recorded along with the applied force (load). The obtained test results are commonly utilized for material selection in quality control applications, as well as to predict the material's response to other types of forces. Based on the recorded values of applied force and elongation, an engineering stress-strain curve was constructed, providing insights into the material's behavior under tensile forces. Ultimately, the outcome of the test was represented by a stress/strain curve, which characterized the material's response to tension.

In-vitro studies

Cell viability and cytotoxicity studies were conducted using the L929 fibroblast cell line obtained from the Pasteur Institute of Iran. The MTT (3-(4,5-dimethylthiazol-2-yl)-2,5-diphenyl tetrazolium bromide) assay was used to assess cell proliferation in the presence of scaffold extracts over a 24-hr period. Absorbance at 545 nm was measured using a microplate reader (STAT-FAX 2100, USA) to determine cell viability. The antibacterial activity of the scaffolds was evaluated against E. coli and Staphylococcus aureus using the disc diffusion method, with the zone of inhibition serving as the indicator. The measurement of antibacterial properties in a substance was conducted using the non-growth zone diameter method. This method involved the dissolution of a specified quantity of isolated bacteria in a serum medium, subsequently cultured as a lawn on Mueller Hinton Agar culture medium. Subsequently, the test samples were placed onto the culture medium. After incubating the plates for 24 hours at 37°C, the plates were examined under light, and the non-growth area was measured.

Fig. 1 (a-c) presents the printed scaffolds, where three different ratios of gelatin solution to chitosan solution are examined. In configuration A, denoted as 1Cs:2G, the gelatin solution is twice the amount of the chitosan solution. Configuration B, labeled as 1Cs:1G, maintains an equal ratio of gelatin solution to chitosan solution. In configuration C, referred to as 1Cs:3G, the gelatin solution is three times the amount of the chitosan solution. Fig. 1 includes a digital camera image depicting the scaffolds printed using the chitosan and gelatin materials. During the sample printing process, the temperature corresponds to the ambient temperature. The printing parameters used are as follows: a printing speed of 120 mm/min, a pressure of 0.6 bar, and a printing plate temperature of -10°C.

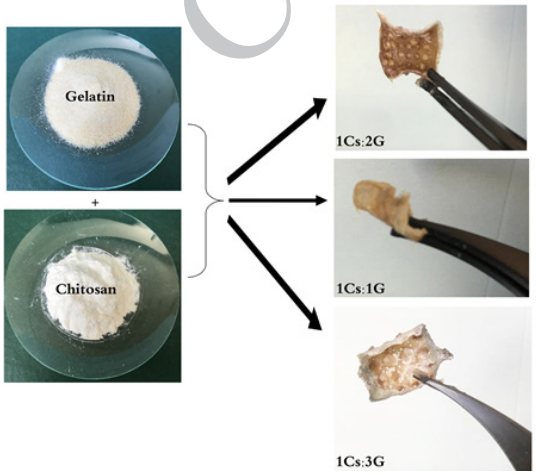

Fig. 1. Digital camera image of scaffolds printed using chitosan and gelatin

Statistical analysis

All the characterization experiments were conducted in triplicate, and the results were presented as the mean ± standard deviation. Statistical analysis was performed using one-way analysis of variance (ANOVA), with a significance level of $P<0.05$.

RESULTS AND DISSCUSIONS

In recent years, tissue engineering has shown great promise in regenerative medicine, with a focus on restoring and replacing damaged tissues and organs. Several studies have explored different aspects of tissue engineering in various applications [32-35]. Iranmanesh et al. [36] investigated the use of 3D bioprinting techniques to enhance the regeneration potential of dental pulp by developing porous architectures in tissue engineering scaffolds. The study emphasized the importance of incorporating porous structures for cell infiltration, nutrient exchange, and tissue integration. Ghomi et al. [37] explored the properties and potential applications of bioactive glass cement and chitosan-gelatin membranes for jawbone tissue engineering, highlighting the importance of understanding biomaterial properties for effective scaffold design. The incorporation of nanoparticles in scaffold materials was also studied by Kheiri Mollaqasem et al. [38], demonstrated the potential of graphene oxide and calcium phosphate nanoparticles in improving the mechanical strength and bioactivity of bone tissue scaffolds. Biazar et al. [39] investigated the effect of mechanical activation on the size reduction of drug particles, providing insights into optimizing drug particle size for enhanced drug delivery efficiency. Khalilimofrad et al. [40] focused on collagen-based electrospun mats for skin tissue engineering, emphasizing material composition and cross-linking techniques.

Dadras et al. [41] and Barbaz-Isfahani et al. [42-43] studied the mechanical properties of composite materials, highlighting the potential of nanoparticles and self-healing polymers to

enhance their behavior. The mechanical behavior of composite materials in harsh environments, such as acidic conditions, was investigated by Dadras et al. [44], while Teimouri et al. [45] explored the effect of core-shell microcapsule sizes on the mechanical properties of microcapsule-based polymers. Finally, Morovvati et al. [46] developed a method to optimize the porosity of porous scaffolds containing magnetic nanoparticles in tissue engineering applications. In order to assess the morphology of the printed scaffolds, both a reflective light microscope and a SEM were utilized [47-52]. A multitude of studies contribute significantly to the field of tissue engineering and regenerative medicine by addressing various aspects of scaffold design, material properties, and application-specific considerations [53-56].

Many studies show valuable insights into the development of innovative materials and techniques for dental and medical applications [57-66]. Fig. 2-A depicts the optical microscope images of the scaffolds, which clearly exhibits a favorable morphology. Fig. 2-B displays the SEM images, revealing that the pores become filled during the printing process due to the material's concentration and viscosity. Consequently,

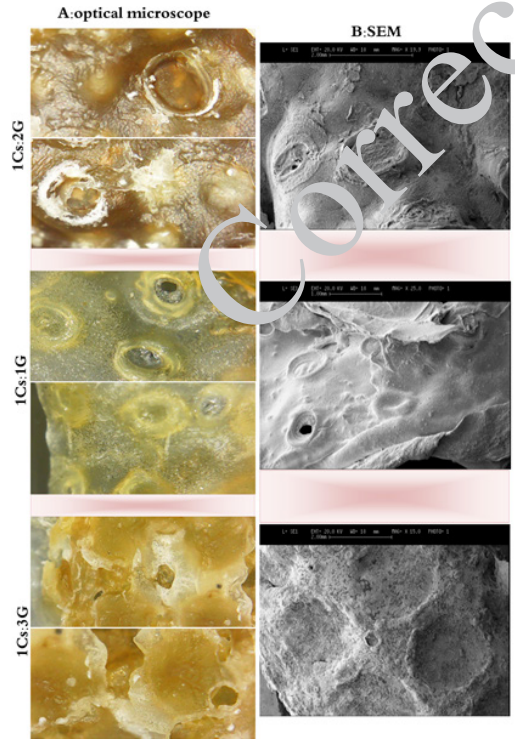

Fig. 2. Examination of morphology using 80x optical microscope and SEM for 3D scaffolds
It is based on SEM image as 30 micron

measuring the strand dimensions becomes impractical. To achieve high-quality printing of the chitosan-based hydrogel, the resolution of the printed scaffold was examined under various settings. The study indicates that the viscoelastic swelling effect of the ink leads to a larger diameter of the extruded strand compared to the nozzle diameter. Furthermore, higher extrusion force (air pressure) intensifies the swelling effect, resulting in a larger diameter of the printed strand at elevated air pressure. Conversely, the strand diameter diminishes at higher printing speeds due to the stretching effect, attributed to volume conservation. Upon closer examination of the morphology, it becomes evident that the 1Cs:1G scaffold exhibits superior pore morphology and transparency compared to the 1Cs:3G and 1Cs:2G scaffolds. This is because the pores are either open or composed of a single, thinly formed layer.

Fig. 3 pertains to the 1Cs:3G scaffold. The observed peaks at 11636 cm^{-1} and 1369 cm^{-1} correspond to the amide I and amide III groups, respectively, which are distinct characteristics of proteins. The absorption regions of O-H exhibit a broad absorption range between 3650 cm^{-1} and 3200 cm^{-1} [36-39], where the vibrations at 3261 cm^{-1} are associated with the O-H functional group. Further analysis of the FTIR spectrum is necessary to elucidate the influence of zinc oxide, crosslinking, and the interplay between the two polymers, as their effects remain unknown.

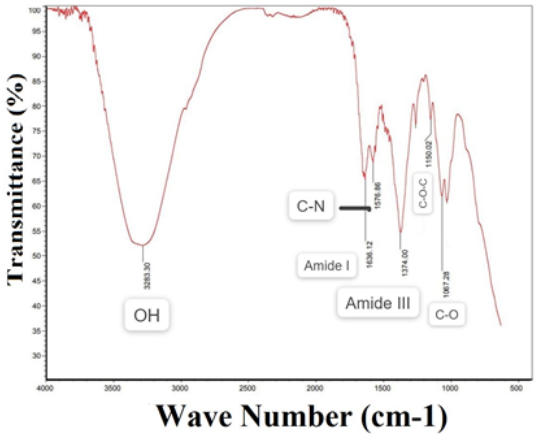

Fig. 3. FTIR spectroscopy of 1Cs:3G

Fig. 4 illustrates the percentage of inflation observed in the scaffolds. The 1Cs:3G scaffold exhibits the highest inflation, reaching 392%. Subsequently, the 1Cs:2G scaffold demonstrates a swelling percentage of 227%, while the inflation for the 1Cs:1G scaffold is reported as 187%. The

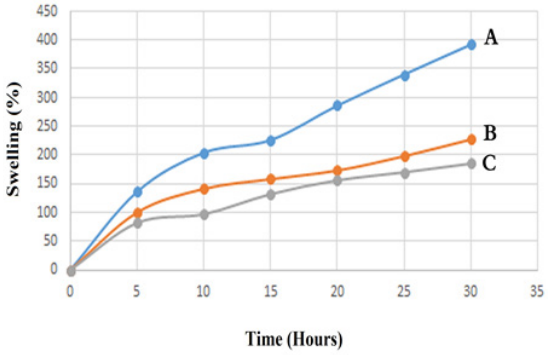

Fig. 4. Swelling percentage diagram of 3D scaffolds without coating, A) 1Cs:3G, B) 1Cs:2G, C) 1Cs:1G

presence of gelatin is identified as the reason for the increased swelling and the variation in swelling percentage compared to other scaffolds. Comparing these three scaffolds, it can be inferred that the percentage of swelling increases with a higher gelatin content. These results substantiate that increasing gelatin content leads to enhanced swelling. Moreover, the results indicate that gelatin and chitosan scaffolds can maintain a stable swelling ability even at a low gelatin/chitosan weight ratio, attributed to stronger intermolecular hydrogen bonds between the gelatin and chitosan scaffolds. These outcomes align with previous studies investigating swelling properties. The primary rationale behind these observations is that the incorporation of gelatin can loosen the structure of the hydrogel membrane, enabling easier spreading of molecular chains within the system.

Fig. 5 shows the degradation process of the coated 3D scaffolds over a period of 15 days. The diagram reveals that the 1Cs:1G/0.5ZnO scaffold exhibits the highest degradation percentage, reaching 58%. The 1Cs:2G/1.5ZnO scaffold shows a degradation percentage of 46%, while the 3D 1Cs:3G/3ZnO scaffold demonstrates the lowest degradation percentage at 38%. The results from the degradation process indicate that an increase

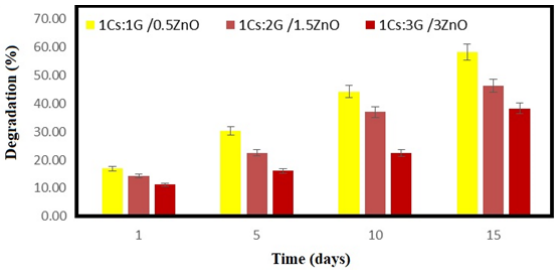

Fig. 5. Biodegradation process of coated three-dimensional scaffolds

in zinc nanoparticles leads to a slower degradation rate. This is attributed to the ability of zinc nanoparticles to reduce water absorption, and as the amount of zinc nanoparticles in the scaffold increases, the water absorption capacity of the scaffold diminishes.

Fig. 6 illustrates the mechanical properties of the coated 3D scaffolds. The chart reveals that the 1Cs:1G/0.5Zn scaffold exhibits the highest tensile strength at 77.07 mm. The tensile strength of the 1Cs:2G/1.5ZnO and 1Cs:2G/3ZnO scaffolds is reported as 60.06 mm and 49.11 mm, respectively. Furthermore, the 1Cs:2G/0.5ZnO scaffold demonstrates the highest Young's modulus at 61.2 MPa. In contrast, the Young's modulus decreases to 2.07 MPa and 1.66 MPa with an increase in zinc nanoparticles.

It can be inferred that the inclusion of zinc nanoparticles in the scaffold may enhance its mechanical properties at lower concentrations. Previous studies have also reported that the incorporation of various nanoparticles in composites can improve mechanical properties up to a certain threshold, beyond which the addition of nanoparticles no longer enhances the mechanical properties [41-35]. The observed increase in tensile strength at lower nanoparticle

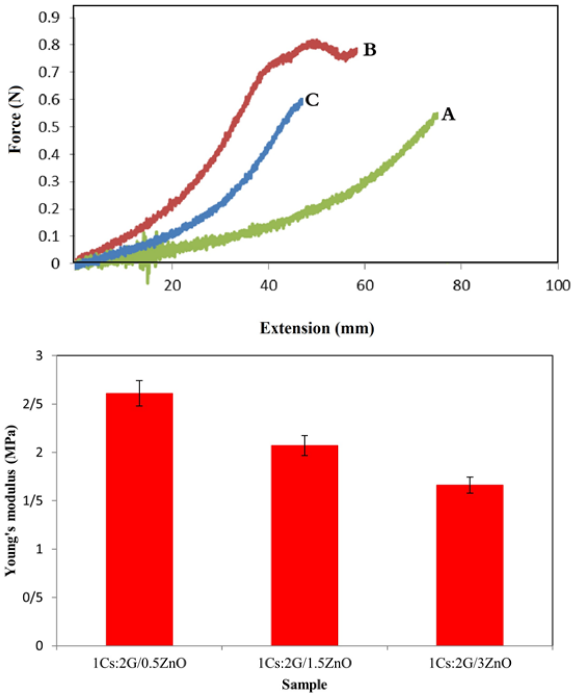

Fig. 6 Investigating the mechanical properties of 3D scaffolds with coating, A) 1Cs:1G/0.5ZnO, B) 1Cs:2G/1.5ZnO, C) 1Cs:1G/3ZnO, D) Young's modulus comparison with diagram 3D scaffold

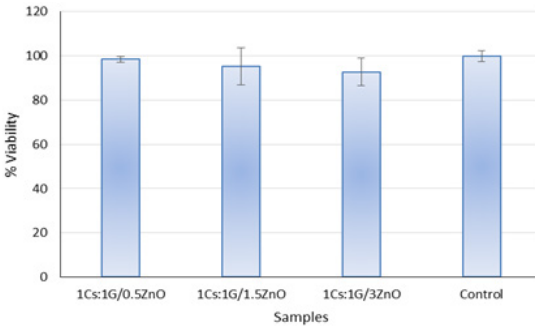

Fig. 7. Survival percentage of fibroblast cells on 3D scaffolds with coating

contents can be attributed to their relatively effective dispersion. Conversely, a higher mass fraction of nanoparticles leads to the formation of clusters and aggregates, introducing defects that ultimately deteriorate the mechanical properties of the scaffold [42-53]. Fig. 7 shows the comparative diagram of cell viability for the 3D scaffolds. The data reveals that there is no significant difference between the 1Cs:1G/0.5ZnO scaffold and the control sample in terms of cell viability. However, there is a significant difference ($P<0.05$) observed between the 1Cs:1G/3ZnO scaffold and both the control sample and the 1Cs:1G/0.5ZnO scaffold.

CONCLUSION

This study focused on the development and evaluation of 3D printed composite scaffolds for tissue engineering applications. The scaffolds were fabricated using chitosan and gelatin materials and incorporated zinc oxide nanoparticles. Coating with sodium alginate was also performed on some scaffolds. Various characterization techniques were employed to assess the morphology, functional groups, swelling, degradation, mechanical properties, and biological performance of the scaffolds, comparing them to uncoated scaffolds. The results indicated that the scaffold with a ratio of 1 part chitosan to 1 part gelatin (1Cs:1G) exhibited optimal morphology and porosity. FTIR confirmed the presence of characteristic peaks for chitosan and gelatin in the scaffolds. Among the coated scaffolds, 1Cs:1G/0.5ZnO scaffold demonstrated the highest swelling (154%), degradation (58%), and mechanical properties. Furthermore, cell viability tests revealed that the 1Cs:1G/0.5ZnO scaffold exhibited the highest cell viability, indicating better biocompatibility compared to other scaffolds. This finding highlights the potential of this scaffold for tissue engineering applications. The study concludes by recommending further investigations, including *in-vivo* tests, optimization of coating materials, and concentration levels. These additional studies can provide deeper insights into the performance and potential of the developed composite scaffolds. This study successfully developed 3D printed chitosan/gelatin/zinc oxide nanoparticle composite scaffolds and demonstrated their potential for tissue engineering applications.

ACKNOWLEDGMENT

I would like to express my sincere gratitude to the Department of Biomedical Engineering at the Science and Research Branch of Islamic Azad University, Tehran, Iran. The support and guidance provided by the faculty and staff have been invaluable throughout my research journey.

AVAILABILITY OF DATA AND MATERIALS

The datasets supporting the conclusions of this study are included within the article.

COMPETING INTERESTS STATEMENT

The authors have declared that no competing interests exist.

FUNDING

None.

REFERENCES

1. Wang Q, Yan J, Yang J, Li B. Nanomaterials promise better bone repair. Mater Today. 2016;19(8):451–463.
2. Basirun WJ, Nasiri-Tabrizi B, Baradaran S. Overview of hydroxyapatite–graphene nanoplatelets composite as bone graft substitute: mechanical behavior and in-vitro biofunctionality. Crit Rev Solid State Mater Sci. 2018;43(3):177–212.
3. Alves Cardoso D, Jansen JA, Leeuwenburgh SC. Synthesis and application of nanostructured calcium phosphate ceramics for bone regeneration. J Biomed Mater Res B Appl Biomater. 2012;100(8):2316–2326.
4. Oryan A, Alidadi S, Moshiri A, Maffulli N. Bone regenerative medicine: classic options, novel strategies, and future directions. J Orthop Surg Res. 2014;9:1–27.
5. Wang N, Dheen ST, Fuh JYH, Kumar AS. A review of multi-functional ceramic nanoparticles in 3D printed bone tissue engineering. Bioprinting. 2021;23:e00146.
6. Xue X, Hu Y, Wang S, Chen X, Jiang Y, Su J. Fabrication of physical and chemical crosslinked hydrogels for bone tissue engineering. Bioact Mater. 2022;12:327–339.
7. Shalumon KT, Anulekha KH, Chennazhi KP, Tamura H, Nair SV, Jayakumar R. Fabrication of chitosan/poly (caprolactone) nanofibrous scaffold for bone and skin tissue engineering. Int J Biol Macromol. 2011;48(4):571–576.
8. Madihally SV, Matthew HW. Porous chitosan scaffolds for tissue engineering. Biomaterials. 1999;20(12):1133–1142.
9. Kim IY, Seo SJ, Moon HS, Yoo MK, Park IY, Kim BC, Cho

CS. Chitosan and its derivatives for tissue engineering applications. Biotechnol Adv. 2008;26(1):1–21.
10. Jayakumar R, Prabaharan M, Kumar PS, Nair SV, Tamura H. Biomaterials based on chitin and chitosan in wound dressing applications. Biotechnol Adv. 2011;29(3):322–337.
11. Djagny KB, Wang Z, Xu S. Gelatin: a valuable protein for food and pharmaceutical industries. Crit Rev Food Sci Nutr. 2001;41(6):481–492.
12. Samadian H, Salehi M, Farzamfar S, Vaez A, Ehterami A, Sahrapeyma H, Ghorbani S. In vitro and in vivo evaluation of electrospun cellulose acetate/gelatin/hydroxyapatite nanocomposite mats for wound dressing applications. Artif Cells Nanomed Biotechnol. 2018;46(sup1):964–974.
13. Gu SY, Wang ZM, Ren J, Zhang CY. Electrospinning of gelatin and gelatin/poly (l-lactide) blend and its characteristics for wound dressing. Mater Sci Eng C. 2009;29(6):1822–1828.
14. Attaeyan A, Shahgholi M, Khandan A. Fabrication and characterization of novel 3D porous Titanium-6Al-4V scaffold for orthopedic application using selective laser melting technique. Iran J Chem Chem Eng. 2024;43(1).
15. Khandan A, Abdellahi M, Ozada N, Ghayour H. Study of the bioactivity, wettability and hardness behaviour of the bovine hydroxyapatite-diopside bio-nanocomposite coating. J Taiwan Inst Chem Eng. 2016;60:538–546.
16. Najafinezhad A, Abdellahi M, Ghayour H, Soheily A, Chami A, Khandan A. A comparative study on the synthesis mechanism, bioactivity and mechanical properties of three silicate bioceramics. Mater Sci Eng C. 2017;72:259–267.
17. Karamian E, Motamedi MRK, Khandan A, Soltani P, Maghsoudi S. An in vitro evaluation of novel NHA/zircon plasma coating on 316L stainless steel dental implant. Prog Nat Sci Mater Int. 2014;24(2):150–156.
18. Moarrefzadeh A, Morovvati MR, Angili SN, Smaisim GF, Khandan A, Toghraie D. Fabrication and finite element simulation of 3D printed poly L-lactic acid scaffolds coated with alginate/carbon nanotubes for bone engineering applications. Int J Biol Macromol. 2023;224:1496–1508.
19. Khandan A, Karamian E, Bonakdarchian M. Mechanochemical synthesis evaluation of nanocrystalline bone-derived bioceramic powder using for bone tissue engineering. Dent Hypotheses. 2014;5(4):155–161.
20. Safaei MM, Abedinzadeh R, Khandan A, Barbaz-Isfahani R, Toghraie D. Synergistic effects of graphene nanosheets and copper oxide nanoparticles on mechanical and thermal properties of composites: Experimental and simulation investigations. Mater Sci Eng B. 2023;289:116248.
21. Karamian E, Abdellahi M, Khandan A, Abdellah S. Introducing the fluorine doped natural hydroxyapatite-titania nanobiocomposite ceramic. J Alloys Compd. 2016;679:375–383.
22. Heydary HA, Karamian E, Poorazizi E, Khandan A, Heydaripour J. A novel nano-fiber of Iranian gum tragacanth-polyvinyl alcohol/nanoclay composite for wound healing applications. Procedia Mater Sci. 2015;11:176–182.
23. Sharafabadi AK, Abdellahi M, Kazemi A, Khandan A, Ozada N. A novel and economical route for synthesizing akermanite (Ca2MgSi2O7) nano-bioceramic. Mater Sci Eng C. 2017;71:1072–1078.
24. Khandan A, Jazayeri H, Fahmy MD, Razavi M. Hydrogels: types, structure, properties, and applications. Biomat Tiss Eng. 2017;4(27):143–69.
25. Khandan A, Ozada N. Bredigite-Magnetite (Ca7MgSi4O16-Fe3O4) nanoparticles: A study on their magnetic properties. J Alloys Compd. 2017;726:729–736.
26. Shayan A, Abdellahi M, Shahmohammadian F, Jabbarzare S, Khandan A, Ghayour H. Mechanochemically aided sintering process for the synthesis of barium ferrite: Effect of aluminum substitution on microstructure, magnetic properties and microwave absorption. J Alloys Compd. 2017;708:538–546.
27. Jabbarzare S, Abdellahi M, Ghayour H, Arpanahi A, Khandan A. A study on the synthesis and magnetic properties of the cerium ferrite ceramic. J Alloys Compd. 2017;694:800–807.
28. Razavi M, Khandan A. Safety, regulatory issues, long-term biotoxicity, and the processing environment. In: Nanobiomaterials Science, Development and Evaluation. Woodhead Publishing; 2017. p. 261–279.
29. Heydary HA, Karamian E, Poorazizi E, Heydaripour J, Khandan A. Electrospun of polymer/bioceramic nanocomposite as a new soft tissue for biomedical applications. J Asian Ceram Soc. 2015;3(4):417–425.
30. Khandan A, Ozada N, Karamian E. Novel microstructure mechanical activated nanocomposites for tissue engineering applications. Bioeng Biomed Sci. 2015;5(1):1.
31. Karimi M, Asefnejad A, Aflaki D, Surendar A, Baharifar H, Saber-Samandari S, Toghraie D. Fabrication of shapeless scaffold reinforced with baghdadite-magnetite nanoparticles using a 3D printer and freeze-drying technique. J Mater Res Technol. 2021;14:3070–3079.
32. Raisi A, Asefnejad A, Shahali M, Doozandeh Z, Kamyab Moghadam B, Saber-Samandari S, Khandan A. A soft tissue fabricated using a freeze-drying technique with carboxymethyl chitosan and nanoparticles for promoting effects on wound healing. J Nanoanalysis. 2020;7(4):262–274.
33. Foroutan S, Hashemian M, Khosravi M, Nejad MG, Asefnejad A, Saber-Samandari S, Khandan A. A porous sodium alginate-CaSiO3 polymer reinforced with graphene nanosheet: fabrication and optimality analysis. Fibers Polym. 2021;22:540–549.
34. Jamnezhad S, Asefnejad A, Motififard M, Yazdekhasti H, Kolooshani A, Saber-Samandari S, Khandan A. Development and investigation of novel alginate-hyaluronic acid bone fillers using freeze drying technique for orthopedic field. Nanomed Res J. 2020;5(4):306–315.
35. Raisi A, Asefnejad A, Shahali M, Sadat Kazerouni ZA, Kolooshani A, Saber-Samandari S, Khandan A. Preparation, characterization, and antibacterial studies of N, O-carboxymethyl chitosan as a wound dressing for bedsore application. Arch Trauma Res. 2020;9(4):181–188.
36. Iranmanesh P, Ehsani A, Khademi A, Asefnejad A, Shahriari S, Soleimani M, Khandan A. Application of 3D bioprinters for dental pulp regeneration and tissue engineering (porous architecture). Transport Porous Med. 2022;142(1):265–293.
37. Ghomi F, Daliri M, Godarzi V, Hemati M. A novel investigation on characterization of bioactive glass cement and chitosan-gelatin membrane for jawbone tissue engineering. J Nanoanalysis. 2021;8(4):292–301.
38. Kheiri Mollaqasem V, Asefnejad A, Nourani MR, Goodarzi V, Kalaee MR. Incorporation of graphene oxide and calcium phosphate in the PCL/PHBV core-shell nanofibers as bone tissue scaffold. J Appl Polym Sci. 2021;138(6):49797.
39. Biazar E, Beitollahi A, Rezayat SM, Forati T, Asefnejad A, Rahimi M, Heidari M. Effect of the mechanical activation on size reduction of crystalline acetaminophen drug particles. Int J Nanomedicine. 2009:283–287.
40. Khalilimofrad Z, Baharifar H, Asefnejad A, Khoshnevisan K. Collagen type I cross-linked to gelatin/chitosan electrospun

mats: Application for skin tissue engineering. Mater Today Commun. 2023;35:105889.
41. Dadras H, Barbaz-Isfahani R, Saber-Samandari S, Salehi M. Experimental and multi-scale finite element modeling for evaluating healing efficiency of electro-sprayed microcapsule based glass fiber-reinforced polymer composites. Polym Compos. 2022; 43(9): 5929-5945.
42. Barbaz-Isfahani R, Dadras H, Taherzadeh-Fard A, Zarezadeh-Mehrizi MA, Saber-Samandari S, Salehi M, et al. Synergistic effects of incorporating various types of nanoparticles on tensile, flexural, and quasi-static behaviors of GFRP composites. FIPO. 2022; 23(7): 2003-2016.
43. Barbaz-Isfahani R, Saber-Samandari S, Salehi M. Multi-scale modeling and experimental study on electrosprayed multicore microcapsule-based self-healing polymers. MAMS. 2022;1-14.
44. Dadras H, Teimouri A, Barbaz-Isfahani R, Saber-Samandari S. Indentation, finite element modeling and artificial neural network studies on mechanical behavior of GFRP composites in an acidic environment. JMR&T. 2023; 24, 5042-5058.
45. Teimouri A, Barbaz Isfahani R, Saber-Samandari S, Salehi M. Experimental and numerical investigation on the effect of core-shell microcapsule sizes on mechanical properties of microcapsule-based polymers. J Compos Mater. 2022;56(18): 2879-2894.
46. Morovvati MR, Angili SN, Saber-Samandari S, Nejad MG, Toghraie D, Khandan A. Global criterion optimization method for improving the porosity of porous scaffolds containing magnetic nanoparticles: Fabrication and finite element analysis. Mater Sci Eng B. 2023; 292, 116414.
47. Sahmani S, Saber-Samandari S, Shahali M, Yekta HJ, Aghadavoudi F, Montazeran AH, et al. Mechanical and biological performance of axially loaded novel bio-nanocomposite sandwich plate-type implant coated by biological polymer thin film. J Mech Behav Biomed Mater. 2018; 88, 238-250.
48. Aghdam HA, Sanatizadeh E, Motififard M, Aghadavoudi F, Saber-Samandari S, Esmaeili S, et al. Effect of calcium silicate nanoparticle on surface texture of calcium phosphates hybrid bio-nanocomposite using for bone substitute application. Powder Technol. 2020; 361, 917-929.
49. Roustazadeh D, Aghadavoudi F, Khandan A. A synergic effect of CNT/Al2O3 reinforcements on multiscale epoxy-based glass fiber composite: fabrication and molecular dynamics modeling. Mol Simul. 2020; 46(16): 1308-1319.
50. Song Y, Ghafari Y, Asefnejad A, Toghraie D. An overview of selective laser sintering 3D printing technology for biomedical and sports device applications: Processes, materials, and applications. Opt Laser Technol. 2024; 171, 110459.
51. Ghafari Y, Asefnejad A, Ogbemudia DO. Gold Nanoparticles in Biomedicine: Advancements in Cancer Therapy, Drug Delivery, Diagnostics, and Tissue Regeneration. Sci Hypo. 2024;1(1).
52. Oudeh Kadhim A, Asefnejad A, Hassanzadeh Nemati N. Fabrication and investigation of 3D scaffold using hydroxyapatite and gelatin nanoparticles for bone cancer treatment with sufficient chemical stability. IJCCE. 2024;43(5):1872-1889.
53. Rajaei A, Kazemian M, Khandan A. Investigation of mechanical stability of lithium disilicate ceramic reinforced with titanium nanoparticles. J Nanomed Res. 2022;7(4):350-359.
54. Khandan A, Nassireslami E, Saber-Samandari S, Arabi N. Fabrication and characterization of porous bioceramic-magnetite biocomposite for maxillofacial fractures application. Dent Hypotheses. 2020; 11(3), 74-85.
55. Mirmohammadi H, Kolahi J, Khandan A. Bibliometric analysis of dental preprints which published in 2022. Dent Hypotheses. 2023;14(1):1-2.
56. Sharifi R, Khazaei S, Mozaffari HR, Amiri SM, Iranmanesh P, Mousavi SA. Effect of massage on the success of anesthesia and infiltration injection pain in maxillary central incisors: Double-blind, crossover trial. Dent Hypotheses. 2017;8(3):61-64.
57. Iranmanesh P, Abedian A, Nasri N, Ghasemi E, Khazaei S. Stress analysis of different prosthesis materials in implant-supported fixed dental prostheses using 3D finite element method. Dent Hypotheses. 2014;5(3):109-114.
58. Mogharehabed A, Behnia H, Nasri N, Iranmanesh P, Gholami SA, Yaghini J. Comparison of the efficacy and side effects of chlorhexidine mouthrinses with (Hexidine) and without (Eramax) alcohol. Dent Hypotheses. 2016;7(3):137-141.
59. Birang R, Yaghini J, Farhad SZ, Shadmehri MA, Afshari Z, Iranmanesh P, Maracy MR, Zadeh AK. Efficacy of Socket-Shield Technique on Tissue Stability of Immediate Implant Placement: A Systematic Review with Meta-Analysis and Trial Sequential Analysis. Dent Hypotheses. 2022;13(3):75-81.
60. Ngoc VT, Ha PT, Hung DT, Anh NV. Management of clear aligner-related severe enamel demineralization with A modified resin infiltration technique: a case report. Dent Hypotheses. 2023;14(2):66-8.
61. Hammadi FR, Abdul-Ameer ZM. Evaluation of the push-out bond strength of the bio-C repair and compare it with the mineral trioxide aggregate and amalgam when used as root-end filling material: an: in vitro: study. Dent Hypotheses. 2023;14(2):62-65.
62. Hassan DH, Al-joranii SM. Effect of feeding pattern and salivary level of growth hormone on the stage of primary tooth eruption: an analytical cross-sectional study. Dent Hypotheses. 2023;14(2):52-54.
63. Karamian E, Khandan A, Kalantar Motamedi MR, Mirmohammadi H. Surface characteristics and bioactivity of a novel natural HA/zircon nanocomposite coated on dental implants. Biomed Res Int. 2014;2014(1):410627.
64. Liang H, Mirinejad MS, Asefnejad A, Baharifar H, Li X, Saber-Samandari S, Toghraie D, Khandan A. Fabrication of tragacanthin gum-carboxymethyl chitosan bio-nanocomposite wound dressing with silver-titanium nanoparticles using freeze-drying method. Mater Chem Phys. 2022;279:125770.
65. Farazin A, Torkpour Z, Dehghani S, Mohammadi R, Fahmy MD, Saber-Samandari S, Labib KA, Khandan A. A review on polymeric wound dress for the treatment of burns and diabetic wounds. Inter J Basic Sci Med. 2021;6(2):44-50.
66. Esmaeili S, Shahali M, Kordjamshidi A, Torkpoor Z, Namdari F, Saber-Samandari S, Nejad MG, Khandan A. An artificial blood vessel fabricated by 3D printing for pharmaceutical application. Nanomed J. 2019;6(3):183-194.